JSHC
Japan Society of
Histochemistry and Cytochemistry
Established 1959

Acta Histochem. Cytochem. 50 (5): 141–147, 2017
doi: 10.1267/ahc.17025

A New Electron Microscopic Method to Observe the Distribution of Phosphatidylinositol 3,4-bisphosphate

Sharmin Aktar[1], Sho Takatori[1,2], Takuma Tsuji[1], Minami Orii[1], Yuki Ohsaki[1], Jinglei Cheng[1] and Toyoshi Fujimoto[1]

[1]Department of Anatomy and Molecular Cell Biology, Nagoya University Graduate School of Medicine, Nagoya 466–8550, Japan and [2]Present affiliation: Laboratory of Neuropathology and Neuroscience, Graduate School of Pharmaceutical Sciences, The University of Tokyo

Received August 29, 2017; accepted September 7, 2017; published online October 7, 2017

Phosphatidylinositol 3,4-bisphosphate [PtdIns(3,4)P_2] is a phosphoinositide that plays important roles in signal transduction, endocytosis, and cell migration among others. The intracellular distribution of PtdIns(3,4)P_2 has mainly been studied by observing the distribution of GFP-tagged PtdIns(3,4)P_2-binding protein domains in live cells and by labeling with anti-PtdIns(3,4)P_2 antibody in fixed cell samples, but these methods only offer low spatial resolution results and may have pitfalls. In the present study, we developed an electron microscopic method to observe the PtdIns(3,4)P_2 distribution using the SDS-treated freeze-fracture replica labeling method. The recombinant GST-tagged pleckstrin homology (PH) domain of TAPP1 was used as the binding probe, and its binding to PtdIns(3,4)P_2 in the freeze-fracture replica was confirmed by using liposomes containing different phosphoinositides and by the lack of labeling by a mutant probe, in which one amino acid in the PH domain was substituted. The method was applied to NIH3T3 cell samples and showed that the increase of PtdIns(3,4)P_2 in cells treated with hydrogen peroxide occurs in the cytoplasmic leaflet of the plasma membrane, except in the caveolar membrane. The present method can define the distribution of PtdIns(3,4)P_2 at a high spatial resolution and will facilitate our understanding of the physiological function of this less studied phosphoinositide.

Key words: phosphatidylinositol 3,4-bisphosphate, electron microscopy, freeze-fracture, hydrogen peroxide, platelet-derived growth factor

I. Introduction

Phosphatidylinositol 3,4-bisphosphate [PtdIns(3,4)P_2] is a phosphoinositide of minor abundance [19]. It was previously assumed to be an intermediate product of PtdIns(3,4,5)P_3 degradation, with no particular significance on its own. However, the presence of phosphatases dedicated to the hydrolysis of PtdIns(3,4)P_2 (i.e., inositol polyphosphate 4-phosphatases [INPP4A and INPP4B]) [3, 25] and proteins specifically binding to PtdIns(3,4)P_2, such as the tandem PH domain-containing proteins (TAPP1 and TAPP2) [16, 21] and lamellipodin/RAPH1 [18], indicated that PtdIns(3,4)P_2 has its own functions. Moreover, PtdIns(3,4)P_2 binds to PtdIns(3,4,5)P_3 effectors, including Akt [7] and 3-phosphoinositide-dependent protein kinase PDK1 [1], with an affinity comparable to PtdIns(3,4,5)P_3. By doing so, it may modulate the PtdIns(3,4,5)P_3-related functionalities of these proteins. Mainly through analyses of the above-mentioned proteins, it is now recognized that PtdIns(3,4)P_2 is involved in a wide range of cellular phenomena, from signal transduction to endocytosis and cell migration [20].

The physiological importance of PtdIns(3,4)P_2 being

Correspondence to: Toyoshi Fujimoto, Department of Anatomy and Molecular Cell Biology, Nagoya University Graduate School of Medicine, 65 Tsurumai, Showa, Nagoya 466–8550, Japan.
E-mail: tfujimot@med.nagoya-u.ac.jp

revealed, the need to determine where and how PtdIns(3,4)P_2 is located in the cell is more urgent than ever. Although methods to quantify the amount of PtdIns(3,4)P_2 in isolated samples have been developed [26], considering the quick time course over which PtdIns(3,4)P_2 is thought to be generated and hydrolyzed, microscopic methods to observe its distribution are essential for understanding PtdIns(3,4)P_2 functions more in detail. In this context, the GFP (or YFP)-tagged pleckstrin homology (PH) domain of TAPP1 was used for live imaging [16, 21], and recombinant TAPP1-PH and anti-PtdIns(3,4)P_2 antibody were used for labeling fixed cells and tissues [5, 15, 31]. Although the results obtained by these methods gave insights into the function of PtdIns(3,4)P_2, the innate problems of those methods have been pointed out [2, 27].

In the present study, we aimed to establish a method to observe the distribution of PtdIns(3,4)P_2 by the quick-freezing and freeze-fracture replica labeling (QF-FRL) technique [9, 11]. In this method, lipids are physically immobilized by freezing followed by freeze-fracture replica formation, and are then labeled for electron microscopic observation. We found that GST-tagged TAPP1-PH labels PtdIns(3,4)P_2 with a higher specificity than a commercially available anti-PtdIns(3,4)P_2 antibody in freeze-fracture replicas. The QF-FRL method using GST-tagged TAPP1-PH as the probe is expected to be useful in delineating the fine distribution of PtdIns(3,4)P_2 in various settings.

II. Materials and Methods

Liposomes

1-palmitoyl-2-oleoyl-sn-glycero-3-phosphocholine (PC) (Nichiyu, Tokyo, Japan) and synthetic dipalmitoylated phosphoinositides (CellSignals, Columbus, OH) were used to prepare liposomes. The lipids were dried in nitrogen gas, hydrated in 20 mM Hepes-NaOH (pH 7.4), and mixed by vortexing. To make unilamellar liposomes, the lipid suspension was passed through a polycarbonate membrane filter with 0.2 μm pores using a Mini-Extruder (Avanti Polar Lipids, Alabaster, AL).

Cell culture

Mouse NIH3T3 cells were maintained in Dulbecco's modified Eagle's medium with high glucose (Sigma-Aldrich, St. Louis, MO) supplemented with 10% (v/v) fetal bovine serum (FBS; Nichirei, Tokyo, Japan) at 37°C in a humidified atmosphere of 95% air and 5% CO_2. For expression of fluorescent biosensors, cells were transfected with cDNA using jetPRIME transfection reagent (Polyplus-transfection, New York, NY) following the manufacturer's instruction. The cells were serum-starved for 16 hr in a medium containing 0.5% FBS before being treated with either 10 mM H_2O_2 or 5 ng/ml recombinant mouse platelet-derived growth factor (PDGF-BB; ProSpec, East Brunswick, NJ).

Probes

The PH domain of TAPP1 (amino acids 182–303) was amplified from HeLa cell cDNA using a forward primer (5'-CGGGATCCTTTTACTCCTAAACCACCTAA-3') and a reverse primer (5'-GGAATTCTCAGGGATGCTCAGAA GACGCAGA-3'), digested with BamHI and EcoRI, and integrated to the pGEX-6P-1 plasmid (GE Healthcare). The mutant probe TAPP1(R211L), in which binding with PtdIns(3,4)P_2 is abrogated by replacement of the 211st arginine of TAPP1 to leucine [6], was generated by polymerase chain reaction using the following primer sets: 5'-GGAGCAGTGATGAAAAACTGGAAGAGACTATATT TTCAATTGG-3' and 5'-CCAATTGAAAATATAGTCTCT TCCAGTTTTTCATCACTGCTCC-3'. GST-tagged recombinant proteins expressed in BL21 *Escherichia coli* cells were purified using glutathione-agarose (Sigma-Aldrich) and dialyzed to phosphate-buffered saline (PBS).

Quick freezing and freeze-fracture replica preparation

Quick freezing and freeze-fracture replica formation were carried out as described previously [4]. In brief, samples sandwiched between a thin copper foil (20 μm) and a flat aluminum disc (Engineering Office M. Wohlwend, Sennwald, Switzerland) were frozen using an HPM 010 high-pressure freezing machine (Leica Microsystems, Wetzler, Germany), and freeze-fracture replicas were prepared in a BAF400 apparatus (BAL-TEC) by electron-beam evaporation in three steps: carbon (2–5 nm in thickness) at an angle of 90° to the specimen surface, platinum-carbon (1–2 nm) at an angle of 45°, and carbon (10–20 nm) at an angle of 90°. Thawed freeze-fracture replicas were treated with 2.5% SDS in 0.1 M Tris-HCl (pH 7.4) at 60°C overnight.

Freeze-fracture replica labeling

Freeze-fracture replicas were washed five times with PBS containing 0.1% Triton X-100 (PBST), blocked with 3% fatty acid-free bovine serum albumin (BSA) and 2% cold fish gelatin (CFG) in PBS for 30 min at room temperature, washed once in PBST, and incubated at 4°C overnight with GST-TAPP1 or GST-TAPP1(R211L) at the concentration of 10 ng/ml in PBS with 1% BSA and 0.67% CFG. The samples were washed five times with PBST, treated with rabbit anti-GST antibody (10 μg/ml; Bethyl Laboratories, Montgomery, TX) in PBS with 1% BSA and 0.67% CFG for 30 min at 37°C, washed five times with PBST, and incubated with protein A conjugated with 5 nm or 10 nm colloidal gold (PAG5, PAG10) (1:50 or 1:60 dilution of the supplied solution; The University Medical Center Utrecht, Utrecht, The Netherlands) in PBS with 1% BSA and 0.67% CFG for 30 min at 37°C. In some experiments, mouse anti-PtdIns(3,4)P_2 antibody (10 μg/ml; Echelon, Salt Lake City, UT) was used instead of GST-TAPP1. After being washed five times with PBST, the replicas were rinsed with distilled water, picked up on Formvar-coated electron microscopy (EM) grids, and observed with a JEOL JEM-1011

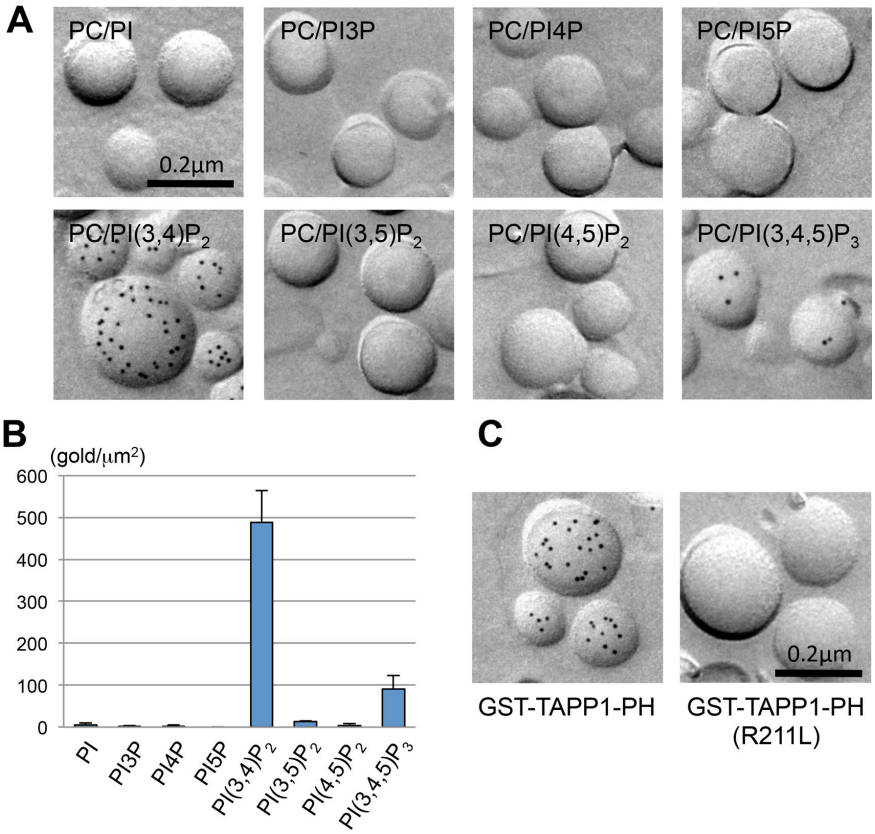

Fig. 1. Labeling of liposomes with GST-TAPP1-PH. **A.** Freeze-fracture replicas of liposomes containing 5 mol% of a phosphoinositide or phosphatidylinositol (PI) and 95 mol% of phosphatidylcholine were labeled with GST-TAPP1-PH. Liposomes containing PtdIns(3,4)P_2 showed by far the most intense labeling. 10 nm gold particles were used. **B.** Quantification of GST-TAPP1-PH labels in the liposome replicas. More than 100 liposomes were randomly chosen and the number of gold particles and the surface area were measured. Mean ± standard error of the mean (SEM) of three independent experiments. **C.** Freeze-fracture replicas of the liposome containing PtdIns(3,4)P_2 were incubated with either 10 ng/ml GST-TAPP1-PH or 10 ng/ml GST-TAPP1-PH(R211L). The labeling was observed only in samples incubated with GST-TAPP1-PH. 10 nm gold particles were used.

EM (Tokyo, Japan) operated at 100 kV. Digital images were captured using a charge-coupled device camera (Gatan, Pleasanton, CA).

Quantitative analysis

The number of colloidal gold particles in EM images was counted manually, and areas were measured using Image J (NIH). The labeling density in the selected structure was calculated by dividing the number of colloidal gold particles by the area. For each structure, the labeling density was measured in ten different micrographs that were taken randomly. Every experiment was repeated more than two times, and a representative result is shown.

III. Results

GST-TAPP1-PH binds to PtdIns(3,4)P_2 in freeze-fracture replicas

In QF-FRL, freeze-fracture replicas physically fix a membrane leaflet, and phospholipids and sphingolipids held in the replicas are labeled with various probes [4, 10, 11, 23, 28]. In applying QF-FRL to a new lipid molecule, it is critical to select an appropriate binding probe, because a probe binding to the target lipid specifically in another modality (e.g., dot blot) does not necessarily bind to the same lipid with a similar specificity in QF-FRL. This is not a problem with QF-FRL alone; similar divergence was also noticed between other methods using lipid-binding probes [24].

In selecting appropriate probes, QF-FRL has an advantage because the binding specificity of probes can be tested without resorting to other methods. That is, whether a probe specifically binds to the target lipid or not can be examined by applying it to freeze-fracture replicas of liposomes with different compositions. In the present study, we prepared liposomes containing 95 mol% phosphatidylcholine (PC) and 5 mol% of a phosphoinositide, and subjected their freeze-fracture replicas to labeling with two probes: one was recombinant GST-tagged TAPP1-PH [31] and the other was mouse anti-PtdIns(3,4)P_2 antibody [5].

By measuring the density of colloidal gold labels in freeze-fracture replicas of liposomes, we found that GST-TAPP1-PH binds to PtdIns(3,4)P_2 with by far the highest intensity (Fig. 1A, B). It also showed binding to

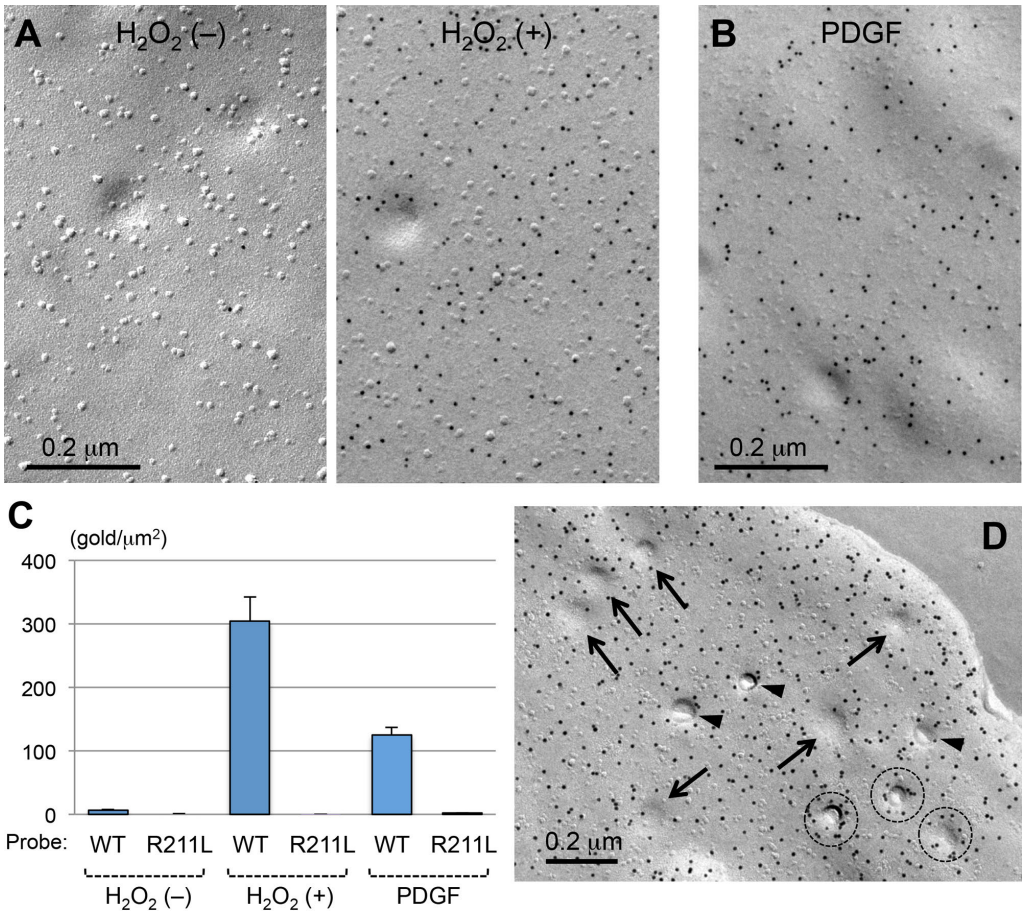

Fig. 2. Labeling of PtdIns(3,4)P_2 in the plasma membrane of NIH3T3 cells. **A.** Labeling of PtdIns(3,4)P_2 in NIH3T3 cells using GST-TAPP1-PH. Cells were either untreated (left) or treated with 10 mM H_2O_2 for 10 min (right). Freeze-fracture replicas of the cytoplasmic leaflet of the plasma membrane are shown. Colloidal gold labels (5 nm) are observed much more densely in H_2O_2-treated samples than in the untreated control, and distribute in the membrane without conspicuous local concentration. **B.** Labeling of PtdIns(3,4)P_2 in NIH3T3 cells that were treated with 5 ng/ml PDGF for 10 min. Significant labeling was observed in the cytoplasmic leaflet of the plasma membrane. 5 nm gold particles were used. **C.** Quantification of PtdIns(3,4)P_2 labels (5 nm gold particles) in the NIH3T3 cell replicas. The freeze-fracture replicas of cells, either untreated, treated with 10 mM H_2O_2 for 10 min, or treated with 5 ng/ml PDGF for 10 min, were incubated with GST-TAPP1-PH or GST-TAPP1-PH(R211L). Ten different areas were randomly chosen, and the number of gold particles per unit membrane area was quantified. Mean ± SEM of one representative experiment is shown. The labeling with GST-TAPP1-PH (shown as WT) increased significantly after the treatment with H_2O_2 or PDGF, whereas that with GST-TAPP1-PH(R211L) was negligible. **D.** Caveolae in NIH3T3 cells treated with 10 mM H_2O_2 for 10 min. The PtdIns(3,4)P_2 label (10 nm gold particles) was not present in the indented area of shallow caveolae (arrows); note that the bottom of deep caveolae could not be seen due to fracturing at their neck (arrowheads and dotted circles). The majority of caveolae did not exhibit particular concentration of the label around them (arrows and arrowheads), whereas some deep caveolae exhibited a denser labeling at the orifice (dotted circles).

PtdIns(3,4,5)P_3, but the labeling intensity to PtdIns(3,4,5)P_3 was much lower than that to PtdIns(3,4)P_2. In contrast, the mouse anti-PtdIns(3,4)P_2 antibody bound to phosphatidylinositol and several phosphoinositides other than PtdIns(3,4)P_2 with significant intensities (Supplementary Fig. 1). It was particularly worrisome that the antibody bound to PtdIns(4,5)P_2 and phosphatidylinositol with high intensities, because the cellular content of those two lipids are much higher than that of PtdIns(3,4)P_2 [19]. We thus used GST-TAPP1-PH as the probe to label PtdIns(3,4)P_2 in subsequent studies.

As the second line of evidence to show the binding specificity of GST-TAPP1-PH, we used a one amino acid-substituted mutant of TAPP1, R211L, that is deficient in binding to PtdIns(3,4)P_2 [6]. It was confirmed that GST-TAPP1-PH(R211L) does not bind to the freeze-fracture replica of PtdIns(3,4)P_2-containing liposomes (Fig. 1C). The result indicated that GST-TAPP1-PH binds to PtdIns(3,4)P_2 in freeze-fracture replicas in the same manner as it does to PtdIns(3,4)P_2 in cells. The mutant probe, GST-TAPP1-PH(R211L) is useful as a negative control to exclude non-specific binding in cellular samples, in which proteins as well as non-tested lipids might show affinity to GST-TAPP1-PH.

Treatment with H_2O_2 and PDGF increases PtdIns(3,4)P_2 in the plasma membrane

PtdIns(3,4)P_2 in culture cells was shown to increase

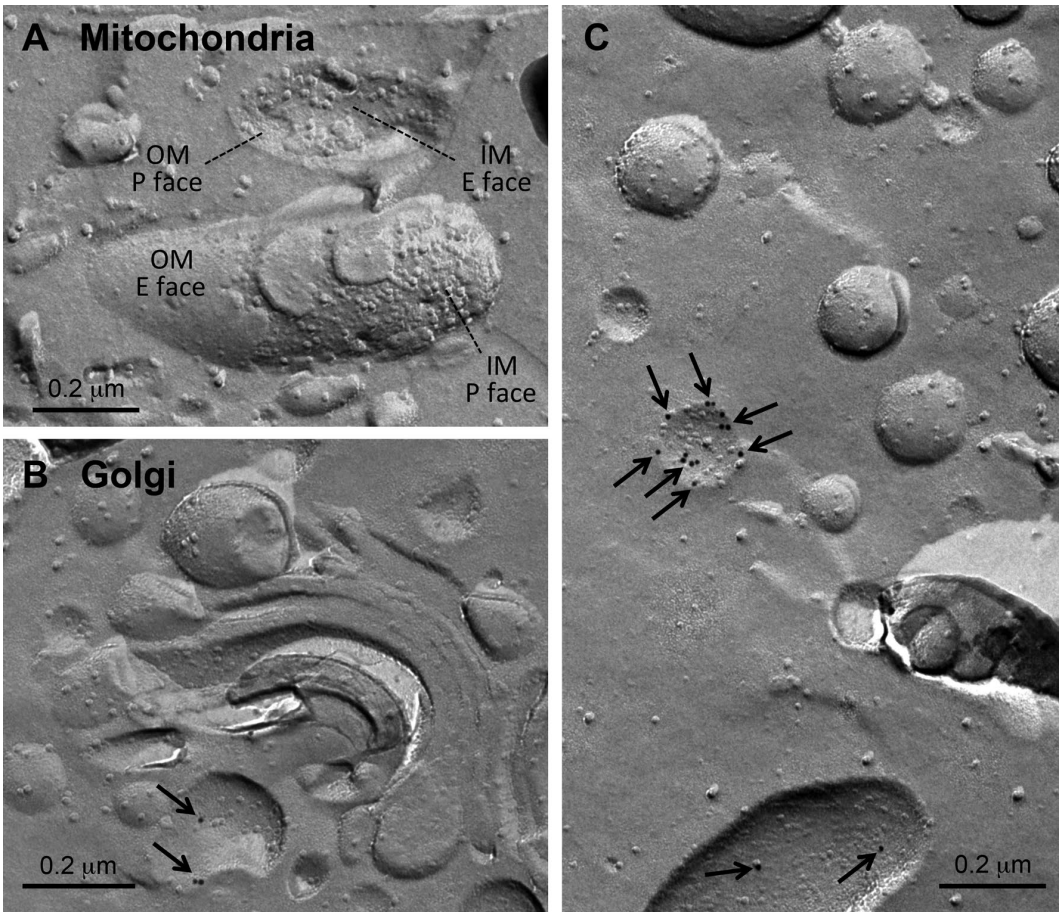

Fig. 3. Labeling of PtdIns(3,4)P_2 in the intracellular organelles of NIH3T3 cells. Labeling of PtdIns(3,4)P_2 in NIH3T3 cells treated with 10 mM H_2O_2 for 10 min. 10 nm gold particles were used. **A.** Mitochondrial membranes. Four membrane leaflets, i.e., the cytoplasmic and non-cytoplasmic leaflets of the outer (OM) and inner (IM) membranes, can be identified in this picture. They were all devoid of labeling. P and E faces correspond to the cytoplasmic and non-cytoplasmic leaflets of the membranes, respectively. **B.** The Golgi membranes. A small number of labels (arrows) were observed in the cytoplasmic leaflet of some membranes. **C.** Some intracellular membranes, which might be the ER, exhibited labeling in the cytoplasmic leaflet (arrows).

significantly upon treatment with H_2O_2 [30] and PDGF [13]. These results were confirmed by live imaging using YFP-TAPP1-PH [16] and by immunoelectron microscopy using recombinant GST-TAPP1-PH [31]. The same studies also showed that PtdIns(3,4)P_2 increases in the plasma membrane upon stimulation [16, 31]. Additionally, the immunoelectron microscopic study suggested an increase of PtdIns(3,4)P_2 in the endoplasmic reticulum (ER) and the internal vesicles of the multivesicular body [31].

We confirmed that H_2O_2 and PDGF increased PtdIns(3,4)P_2 in the plasma membrane of NIH3T3 cells by observing the distribution of expressed GFP-TAPP1-PH by fluorescence microscopy (data not shown). In this cell type, the obvious distributional change of GFP-TAPP1-PH (i.e., from diffuse cytosolic to cell periphery) with H_2O_2 occurred only when it was used at 10 mM. Therefore, NIH3T3 cells treated with 10 mM H_2O_2 for 10 min and those treated with 5 ng/ml PDGF for 10 min were examined in subsequent experiments.

When NIH3T3 cells were quick-frozen without applying any reagent, the labeling for PtdIns(3,4)P_2 in the freeze-fracture replica was scarce either in the plasma membrane or in any other cellular membranes (Fig. 2A, left). After stimulation with H_2O_2 for 10 min, intense labeling was observed in the cytoplasmic leaflet of the plasma membrane (Fig. 2A, right). Treatment with PDGF for 10 min also increased the PtdIns(3,4)P_2 labeling in the cytoplasmic leaflet of the plasma membrane (Fig. 2B). Although variation among cells was observed in both experiments, the average labeling density in the plasma membrane increased approximately 45-fold and 18-fold after the treatment with H_2O_2 and PDGF, respectively (Fig. 2C).

The PtdIns(3,4)P_2 labeling in the plasma membrane of cells after treatment with H_2O_2 or PDGF was distributed without prominent local variation. It is of note, however, that the labeling largely spared the membrane of shallow caveolae, whereas a small population of deep caveolae showed dense labeling at their orifice (Fig. 2D). The shallow and deep caveolae can be identified by morphology alone, but their identity was further confirmed by immunolabeling for caveolin-1 (Supplementary Fig. 2) [8]. This distribution pattern of PtdIns(3,4)P_2 labeling was different

from that of phosphatidylinositol 4,5-bisphosphate, which shows concentration in both deep and shallow caveolae [11]. Binding of cavins is thought to stabilize deep caveolae invagination [17], but it is not clear whether generation of deep and shallow caveolae is dictated solely by cavins. It would be interesting to study if phosphatidylinositols play any role in the definition of caveolae depth.

Importantly, the mutant probe, GST-TAPP1-PH(R211L), did not show labeling in either unstimulated or stimulated cellular samples (Fig. 2C, Supplementary Fig. 3), indicating that the label obtained with GST-TAPP1-PH was derived from PtdIns(3,4)P_2, and not caused by nonspecific binding.

We also observed intracellular membranes of the stimulated cells by QF-FRL. In H_2O_2-treated cells, the inner and outer mitochondrial membranes were devoid of PtdIns(3,4)P_2 labeling (Fig. 3A) whereas membranes in the Golgi occasionally showed a low level of labeling (Fig. 3B). Additionally, some vesicular structures were labeled in the cytoplasmic leaflet (Fig. 3C), but the identity of those structures could not be determined by morphological criteria. In view of the previous report that showed an increase of PtdIns(3,4)P_2 in the ER membrane after the H_2O_2 treatment [31], they might represent the ER membrane. Cells after the PDGF treatment gave similar results (data not shown).

IV. Discussion

The present study showed that QF-FRL can label PtdIns(3,4)P_2 using recombinant GST-TAPP1-PH as the probe. In comparison to EM methods using ultrathin sections, an advantage of freeze-fracture EM is that membranes can be observed in two-dimensional planes. Because the method can visualize PtdIns(3,4)P_2 distribution in a high spatial resolution, it is expected to be useful to analyze phenomena occurring in small areas of membranes.

Additionally, the QF-FRL method appears to label PtdIns(3,4)P_2 more efficiently than the method using sections: the increase of PtdIns(3,4)P_2 labeling after stimulation with H_2O_2 and PDGF was approximately 45-fold and 18-fold (per unit area of the plasma membrane), respectively, by QF-FRL, whereas by methods using sections, the increase (per unit length of the plasma membrane) was approximately four-fold and 2- to 2.5-fold when PtdIns(3,4)P_2 was directly labeled [31] and approximately 10.4-fold and 5.2-fold when expressed GFP-TAPP1-PH was labeled [16]. The result of QF-FRL agrees better with the drastic increase of PtdIns(3,4)P_2 that was measured biochemically [13, 30].

Efficient labeling, or a high capture ratio, of QF-FRL was also noticed in the labeling of other membrane lipids [4, 10, 11]. One of the reasons for this efficiency is that freeze-fracture replicas can hold membrane lipids physically [12]. Despite the extensive SDS treatment, a model study using liposomes showed that no less than 80% of phospholipids are retained in the replica [12]. In contrast, chemical fixation using aldehydes does not work on most lipids [29] so redistribution of lipids may occur even after fixation [4, 14, 22]. We argue that physical fixation provided by freeze-fracture replicas is crucial for retaining membrane lipids for various analyses [27].

On the other hand, freeze-fracture EM has several problems. One is the difficulty in identifying some subcellular structures, as exemplified by the ER membrane in the present study. Another is the difficulty of observing long protrusions and deep indentations in their entirety because the fracture plane tends to run horizontally, that is, along flat membranes [9]. Furthermore, it is not clear whether the retention of lipids occurs with the same efficiency in membranes of different curvatures, and steric hindrance between probes poses a problem when the labeling density is high [27]. More specifically, on the present method, it needs to be reminded that a non-negligible level of binding may occur with PtdIns(3,4,5)P_3. Despite these problems, however, we believe that the method using TAPP1-PH for freeze-fracture replica labeling is an important tool that can be employed to analyze PtdIns(3,4)P_2 in various cellular context.

V. Conflicts of Interest

The authors declare no conflicts of interest.

VI. Author Contributions

TF conceived and designed the experiments; SA, ST, TT, YO and JC performed the experiments; SA, TT, MO, JC and TF analyzed the data; SA and TF wrote the paper.

VII. Acknowledgments

The authors are grateful to Ms. Tsuyako Tatematsu for her excellent technical assistance. ST was a research fellow of the Japan Society for the Promotion of Science (JSPS) when the major part of this study was done. This work was supported by a Grant-in-Aid for JSPS Fellows (12J10940), Grants-in-Aid for Young Scientists (B) from JSPS (26860132 to ST and 17K15544 to TT), Grants-in-Aid for Scientific Research (15H2500 and 15H05902 to TF).

VIII. References

1. Alessi, D. R., James, S. R., Downes, C. P., Holmes, A. B., Gaffney, P. R., Reese, C. B. and Cohen, P. (1997) Characterization of a 3-phosphoinositide-dependent protein kinase which phosphorylates and activates protein kinase Balpha. *Curr. Biol.* 7; 261–269.
2. Balla, T. (2007) Imaging and manipulating phosphoinositides in living cells. *J. Physiol.* 582; 927–937.
3. Bansal, V. S., Caldwell, K. K. and Majerus, P. W. (1990) The isolation and characterization of inositol polyphosphate 4-phosphatase. *J. Biol. Chem.* 265; 1806–1811.

4. Cheng, J., Fujita, A., Yamamoto, H., Tatematsu, T., Kakuta, S., Obara, K., Ohsumi, Y. and Fujimoto, T. (2014) Yeast and mammalian autophagosomes exhibit distinct phosphatidylinositol 3-phosphate asymmetries. *Nat. Commun.* 5; 3207.
5. Chiang, H. C., Wang, L., Xie, Z., Yau, A. and Zhong, Y. (2010) PI3 kinase signaling is involved in Abeta-induced memory loss in Drosophila. *Proc. Natl. Acad. Sci. U S A* 107; 7060–7065.
6. Dowler, S., Currie, R. A., Campbell, D. G., Deak, M., Kular, G., Downes, C. P. and Alessi, D. R. (2000) Identification of pleckstrin-homology-domain-containing proteins with novel phosphoinositide-binding specificities. *Biochem. J.* 351; 19–31.
7. Franke, T. F., Kaplan, D. R., Cantley, L. C. and Toker, A. (1997) Direct regulation of the Akt proto-oncogene product by phosphatidylinositol-3,4-bisphosphate. *Science* 275; 665–668.
8. Fujimoto, T. and Fujimoto, K. (1997) Metal sandwich method to quick-freeze monolayer cultured cells for freeze-fracture. *J. Histochem. Cytochem.* 45; 595–598.
9. Fujita, A., Cheng, J. and Fujimoto, T. (2010) Quantitative electron microscopy for the nanoscale analysis of membrane lipid distribution. *Nat. Protoc.* 5; 661–669.
10. Fujita, A., Cheng, J., Hirakawa, M., Furukawa, K., Kusunoki, S. and Fujimoto, T. (2007) Gangliosides GM1 and GM3 in the living cell membrane form clusters susceptible to cholesterol depletion and chilling. *Mol. Biol. Cell* 18; 2112–2122.
11. Fujita, A., Cheng, J., Tauchi-Sato, K., Takenawa, T. and Fujimoto, T. (2009) A distinct pool of phosphatidylinositol 4,5-bisphosphate in caveolae revealed by a nanoscale labeling technique. *Proc. Natl. Acad. Sci. U S A* 106; 9256–9261.
12. Fujita, A. and Fujimoto, T. (2007) Quantitative retention of membrane lipids in the freeze-fracture replica. *Histochem. Cell Biol.* 128; 385–389.
13. Gray, A., Van Der Kaay, J. and Downes, C. P. (1999) The pleckstrin homology domains of protein kinase B and GRP1 (general receptor for phosphoinositides-1) are sensitive and selective probes for the cellular detection of phosphatidylinositol 3,4-bisphosphate and/or phosphatidylinositol 3,4,5-trisphosphate in vivo. *Biochem. J.* 344; 929–936.
14. Heffer-Lauc, M., Lauc, G., Nimrichter, L., Fromholt, S. E. and Schnaar, R. L. (2005) Membrane redistribution of gangliosides and glycosylphosphatidylinositol-anchored proteins in brain tissue sections under conditions of lipid raft isolation. *Biochim. Biophys. Acta* 1686; 200–208.
15. Irino, Y., Tokuda, E., Hasegawa, J., Itoh, T. and Takenawa, T. (2012) Quantification and visualization of phosphoinositides by quantum dot-labeled specific binding-domain probes. *J. Lipid Res.* 53; 810–819.
16. Kimber, W. A., Trinkle-Mulcahy, L., Cheung, P. C., Deak, M., Marsden, L. J., Kieloch, A., Watt, S., Javier, R. T., Gray, A., Downes, C. P., Lucocq, J. M. and Alessi, D. R. (2002) Evidence that the tandem-pleckstrin-homology-domain-containing protein TAPP1 interacts with Ptd(3,4)P2 and the multi-PDZ-domain-containing protein MUPP1 in vivo. *Biochem. J.* 361; 525–536.
17. Kovtun, O., Tillu, V. A., Ariotti, N., Parton, R. G. and Collins, B. M. (2015) Cavin family proteins and the assembly of caveolae. *J. Cell Sci.* 128; 1269–1278.
18. Krause, M., Leslie, J. D., Stewart, M., Lafuente, E. M., Valderrama, F., Jagannathan, R., Strasser, G. A., Rubinson, D. A., Liu, H., Way, M., Yaffe, M. B., Boussiotis, V. A. and Gertler, F. B. (2004) Lamellipodin, an Ena/VASP ligand, is implicated in the regulation of lamellipodial dynamics. *Dev. Cell* 7; 571–583.
19. Lemmon, M. A. (2008) Membrane recognition by phospholipid-binding domains. *Nat. Rev. Mol. Cell Biol.* 9; 99–111.
20. Li, H. and Marshall, A. J. (2015) Phosphatidylinositol (3,4) bisphosphate-specific phosphatases and effector proteins: A distinct branch of PI3K signaling. *Cell. Signal.* 27; 1789–1798.
21. Marshall, A. J., Krahn, A. K., Ma, K., Duronio, V. and Hou, S. (2002) TAPP1 and TAPP2 are targets of phosphatidylinositol 3-kinase signaling in B cells: sustained plasma membrane recruitment triggered by the B-cell antigen receptor. *Mol. Cell. Biol.* 22; 5479–5491.
22. Mobius, W., Ohno-Iwashita, Y., van Donselaar, E. G., Oorschot, V. M., Shimada, Y., Fujimoto, T., Heijnen, H. F., Geuze, H. J. and Slot, J. W. (2002) Immunoelectron microscopic localization of cholesterol using biotinylated and non-cytolytic perfringolysin O. *J. Histochem. Cytochem.* 50; 43–55.
23. Murate, M., Hayakawa, T., Ishii, K., Inadome, H., Greimel, P., Watanabe, M., Nagatsuka, Y., Ito, K., Ito, Y., Takahashi, H., Hirabayashi, Y. and Kobayashi, T. (2010) Phosphatidylglucoside forms specific lipid domains on the outer leaflet of the plasma membrane. *Biochemistry* 49; 4732–4739.
24. Narayan, K. and Lemmon, M. A. (2006) Determining selectivity of phosphoinositide-binding domains. *Methods* 39; 122–133.
25. Norris, F. A., Auethavekiat, V. and Majerus, P. W. (1995) The isolation and characterization of cDNA encoding human and rat brain inositol polyphosphate 4-phosphatase. *J. Biol. Chem.* 270; 16128–16133.
26. Sarkes, D. A. and Rameh, L. E. (2016) Analysis of the phosphoinositide composition of subcellular membrane fractions. *Methods Mol. Biol.* 1376; 213–227.
27. Takatori, S., Mesman, R. and Fujimoto, T. (2014) Microscopic methods to observe the distribution of lipids in the cellular membrane. *Biochemistry* 53; 639–653.
28. Takatori, S., Tatematsu, T., Cheng, J., Matsumoto, J., Akano, T. and Fujimoto, T. (2016) Phosphatidylinositol 3,5-bisphosphate-rich membrane domains in endosomes and lysosomes. *Traffic* 17; 154–167.
29. Tanaka, K. A., Suzuki, K. G., Shirai, Y. M., Shibutani, S. T., Miyahara, M. S., Tsuboi, H., Yahara, M., Yoshimura, A., Mayor, S., Fujiwara, T. K. and Kusumi, A. (2010) Membrane molecules mobile even after chemical fixation. *Nat. Methods* 7; 865–866.
30. Van der Kaay, J., Beck, M., Gray, A. and Downes, C. P. (1999) Distinct phosphatidylinositol 3-kinase lipid products accumulate upon oxidative and osmotic stress and lead to different cellular responses. *J. Biol. Chem.* 274; 35963–35968.
31. Watt, S. A., Kimber, W. A., Fleming, I. N., Leslie, N. R., Downes, C. P. and Lucocq, J. M. (2004) Detection of novel intracellular agonist responsive pools of phosphatidylinositol 3,4-bisphosphate using the TAPP1 pleckstrin homology domain in immunoelectron microscopy. *Biochem. J.* 377; 653–663.